

Polytetrafluoroethylene-Based Solvent-Free Procedure for Lithium-Ion Batteries Manufacturing

Subjects: Materials Science, Composites

Contributor: Xuehan Wang, Shuli Chen, Kaiqi Zhang, Licheng Huang, Huilin Shen, Zheng Chen, Changru Rong, Guibin Wang, Zhenhua Jiang

Lithium-ion batteries (LIBs) have become popular for energy storage due to their high energy density, storage capacity, and long-term cycle life. Although binders make up only a small proportion of LIBs, they have become the key to promoting the transformation of the battery preparation process. Along with the development of binders, the battery manufacturing process has evolved from the conventional slurry-casting (SC) process to a more attractive solvent-free (SF) method. Compared with traditional LIBs manufacturing method, the SF method could dramatically reduce and increase the energy density due to the reduced preparation steps and enhanced electrode loading. Polytetrafluoroethylene (PTFE), as a typical binder, has played an important role in fabricating high-performance LIBs, particularly in regards to the SF technique.

Keywords: lithium-ion battery (LIBs) ; polymer binder ; solvent-free (SF) procedure ; polytetrafluoroethylene (PTFE)

1. Introduction

With the increasing global energy consumption, it is urgent to investigate alternative low-carbon and ecologically friendly energy sources to minimize reliance on fossil fuels and meet the rising demand for energy storage ^{[1][2][3][4]}. Lithium-ion batteries (LIBs) ^{[4][5]} are one of the most promising energy technologies. They are rapidly gaining popularity in new energy vehicles, intelligent gadgets, and electronic devices due to their high energy density, excellent efficiency, and long cycle life ^{[6][7][8]}. However, while LIBs present opportunities, they also reveal significant inherent challenges. Previous work ^{[9][10]} has shown that the electrode preparation process significantly affects the performance and capability of LIBs. Their manufacturing costs and the pollution emitted by recycling waste batteries require further reduction.

Currently, the slurry-casting (SC) process is used to prepare most commercialized LIBs electrodes ^{[11][12]}. First, the active material, conductive agent, and binder are homogeneously mixed under solvent-free conditions; then, deionized water ^[12] or N-methyl pyrrolidone (NMP) ^{[13][14]}, etc., solvent is added to prepare a slurry with suitable viscosity for casting on the electrode collector; after that, the slurry is coated on the electrode collector; and finally, the finished electrodes are produced by heating, rolling, and other processes. However, there are several problems with the SC process. (1) Energy consumption for solvent evaporation. Solvents such as NMP have to be dried using large production lines for rapid evaporation from SC electrodes. The total energy consumption is 51% of the production line using 1 million batteries (20.5 Ah, 3.7 V) per year ^[15].

2. Developments in SF Processes and Binders

2.1. SF Processes

With the progressive realization of the significant advantages of the SF process, various SF electrode processes have evolved and have been employed in the fabrication of LIBs. As shown in **Figure 1a–f**, there are six typical SF electrode manufacturing processes: dry spraying deposition ^{[11][16][17]}, vapor deposition ^{[18][19]}, melting and extrusion ^[20], 3D printing ^{[21][22]}, direct pressing ^{[23][24]}, and polymer fibrillation ^{[25][26][27]}.

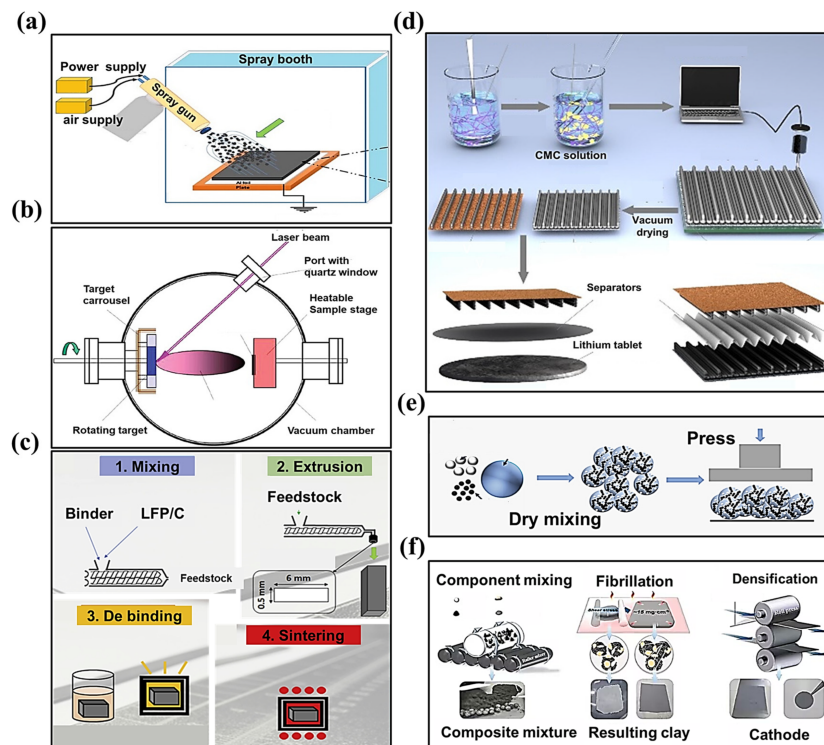


Figure 1. SF electrode manufacturing processes of (a) dry spraying deposition ^[17], (b) vapor deposition ^{[18][19]}, (c) melting and extrusion ^[20], (d) 3D printing ^{[21][22]}, (e) direct pressing ^{[23][24]}, and (f) polymer fibrillation ^{[25][26][27]}.

I. Dry spray deposition

As shown in **Figure 1a**, the method involves the dry mixing of the active material and the conductive agent first; then, the composite powder obtained is added to the spraying device. The composite powder (active material, conductive agent, binder) is sprayed onto the collector through the spraying device and then reinforced using the heat pressing method. For this method, the PVDF binder, or PVDF binder with a certain percentage of PTFE added, are commonly used ^[28].

II. Vapor deposition

This method vaporizes and deposits materials onto a substrate, and the process includes atomic layer deposition, magnetron sputtering, and pulsed laser deposition ^{[18][19]}. This method can prepare electrodes with a high energy density and a long cycle life. However, the equipment required for this method is complex, and the operating environment requires the use of a vacuum.

III. Melting and extrusion

This method is suitable for the preparation of a solid polymer electrolyte, which is widely used in the melt mixing of thermoplastics or ceramic slurry mixing. Although this method can prepare highly loaded electrodes, the process is sensitive to particle size and requires precise control of the extrusion temperature, shear force, and extrusion time. In addition, this method precludes its application in industrial manufacturing due to the cumbersome manufacturing process and the high de-binding and sintering temperatures.

IV. 3D printing

This method fabricates electrodes using a fused deposition modeling (FDM) mechanism in which layers of molten polymer material are stacked horizontally using a specific nozzle tip. The freestanding electrodes produced by this method exhibit a specific morphology, and the thickness may be customized according to the specific application situations. Nevertheless, this technique cannot be applied to fabricate electrodes on a large scale; instead, it can only be used for specific scenarios, such as in the production of microelectronics and wearable devices.

V. Direct pressing

Direct pressing is also known as powder compacting, which is a direct method for pressing powder into shape. It is appropriate for preparing electrolytes and electrodes for all-solid-state batteries. As shown in **Figure 1e**, this method is

simpler and more efficient compared to other methods. Nonetheless, this method exhibits the disadvantage of showing uneven stress and density distribution during unidirectional pressing.

VI. Polymer fibrillation

The process steps include four steps: (i) dry powder mixing, (ii) binder proto-fibrillation, (iii) self-supporting membrane molding, and (iv) self-supporting membrane composite formation, with a collector [28]. In this method, a polymer binder capable of forming a fibrous structure under the action of shear force is employed to achieve an effective connection between the electrode active particles and the conductive additives and other substances. The PTFE possesses significant fibrillar characteristics and highly stable thermo-mechanical properties. Therefore, most of the processes select PTFE as the binder in the polymer fibrillation method.

In addition, two common electrode molding processes [29] include powder extrusion molding and powder roll molding, as shown in **Figure 2a,b**. Powder extrusion molding refers to the micro-fibrillated mixed powder created using a twin-screw extruder to increase high-speed shear to create the fibrillated binder and form it into a self-supporting film and a collector for the composite. Powder roll forming refers to the fibrillation of the mixed powder using a multi-stage roller press incorporating a differential shear roller pressing process so that the binder fibrillation and preparation of the self-supporting membrane can occur, followed by the production of the composite with the collector [29].

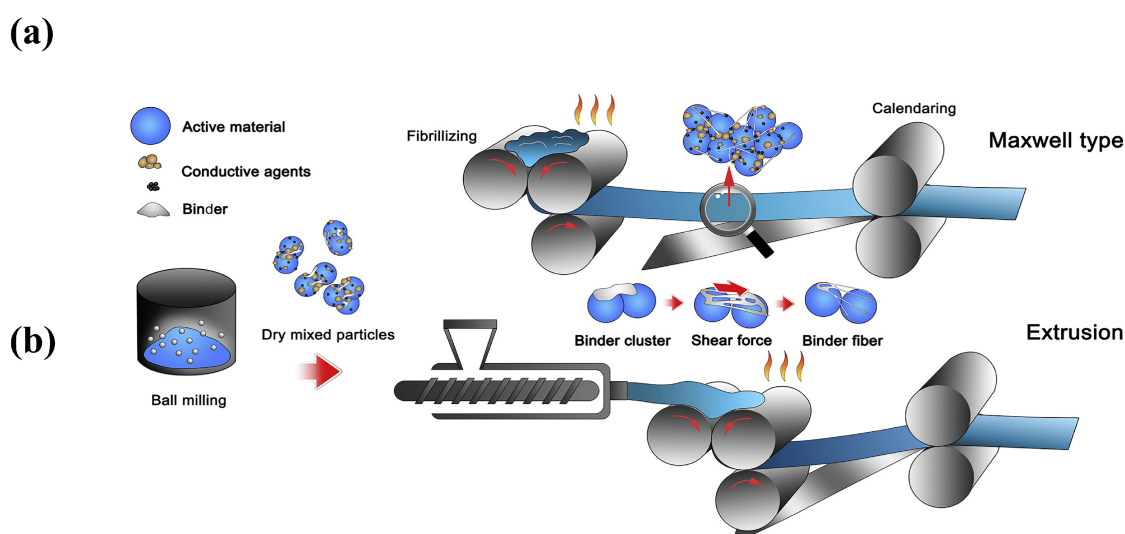


Figure 2. Processes of (a) powder extrusion molding, and (b) powder roll molding [29].

2.2. Binders

Actually, the SF process shows a tight relationship with the binder. The battery binder is a class of polymer compounds that adheres the active materials and conductive agents in the electrode sheet to the electrode collector, and it is one of the essential constituent materials of LIBs [13][30]. Although the amount of binder is small (~5 wt%) [31], it serves to enhance the contact between the active material, the conductive agent, and the collector, as well as to stabilize the structure of the electrode sheet, which determines the change of the fabrication technology. Typical binders used in LIBs electrodes include PVDF [32][33][34][35][36][37], PTFE, styrene-butadiene rubber (SBR) [38][39][40], sodium carboxymethylcellulose (CMC) [41][42][43], poly (acrylic acid) (PAA) [44][45], poly (ethylene oxide) (PEO) [46][47][48], alginate [49][50][51], etc.

In 2023, Tian Qin et al. [52] summarized the adhesion, tensile strength, elasticity, swelling, conductivity, thermal stability, and oxidation stability of seven types of binders. Among them, PVDF, as the major binder for commercial battery systems (cathode), shows the most satisfactory balance between the material and electrochemical properties, as shown in **Figure 3**.

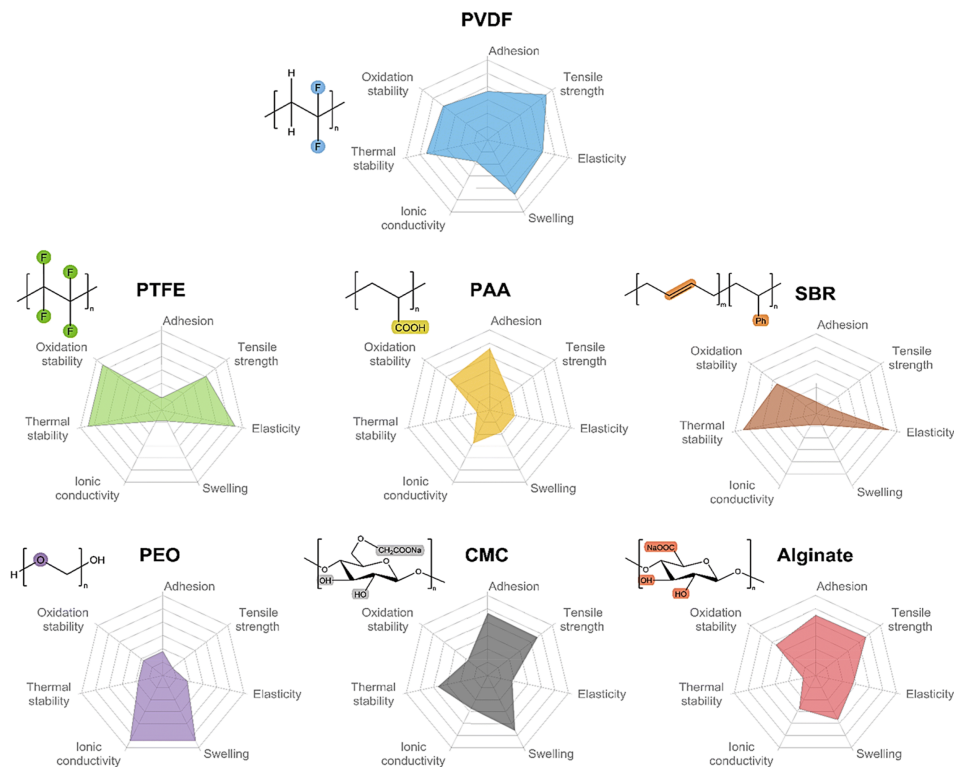


Figure 3. Comparison of the basic properties of common binders.

The mechanical properties of CMC, PAA, and alginate are inferior to those of PVDF; however, they are rich in polar groups such as carboxylic or hydroxyl groups. The free carboxylic acid groups are able to interact with the hydroxyl groups on the surface of materials such as silicon/carbon and aluminum foils, resulting in better bonding properties. Even though CMC is inexpensive and thermally stable, it exhibits high rigidity and brittleness. In order to resolve these issues, CMC is often used as an anode binder in conjunction with SBR, which has high elasticity. The silicon anode with the SBR-CMC composite binder showed a smaller Young's modulus and stronger adhesion strength to the collector [53]. PTFE, SBR, CMC, PAA, etc., could be used with water as a solvent to reduce the toxicity associated with the use of organic solvents, whereas further optimization of the time-consuming and energy-consuming drying step is still necessary in order to decrease the cost of battery manufacturing.

Based on the above considerations, researchers have continued to explore new electrode fabrication methods that do not require the use of solvents. Spray deposition and polymer fibrillation are considered as the two most mainstream methods for the fabrication of SF electrode membranes [28][54]. PVDF is mainly used as binder in the spray deposition method [55], and the binders of polymer fibrillation include PTFE, ethylene-tetra-fluoro-ethylene (ETEF), and fluorinated ethylene propylene (FEP) [28].

3. Binders of PTFE

3.1. Aqueous Binders of PTFE

Currently, most cathode binders use the PVDF [30]. However, the NMP solvent is expensive and harmful to organisms and the environment [56]. Water-based binder performs equally as well as, or even better than, oil-based binder. Choosing the right amount of water-based binder could improve the behavior of the battery. Therefore, many companies are actively exploring the use of cheaper and more environmentally friendly water-based binders to replace PVDF. The PTFE binder shows extraordinary suitability for LIBs due to its excellent mechanical properties, electrochemical ability, and electrolyte compatibility [57]. In addition, PTFE could form an emulsion in aqueous solution containing stabilizers. In recent years, several studies have been conducted using aqueous bonding agents for PTFE. For instance, Gao et al. [58] applied a PTFE aqueous binder in the creation of C/LiFePO₄ batteries. The SEM images of electrodes prepared using PTFE and PVDF are shown in **Figure 4**.

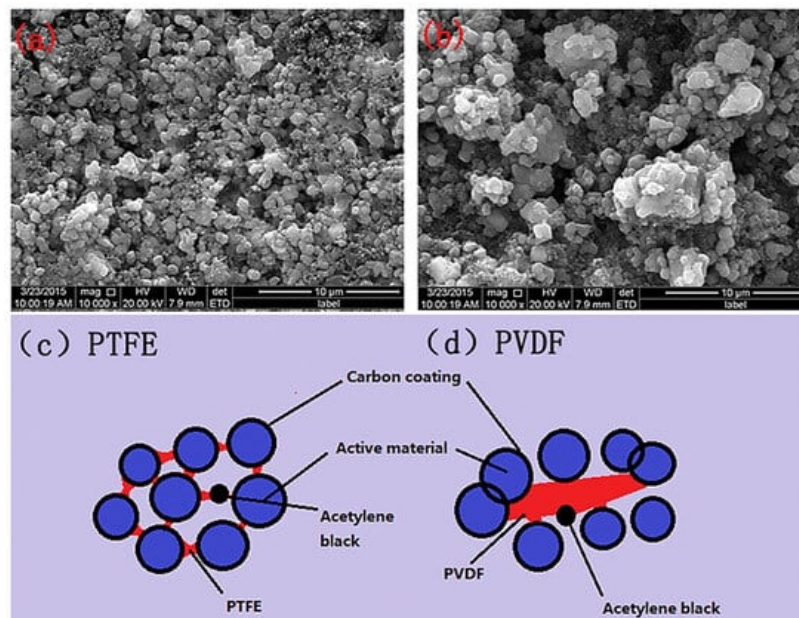


Figure 4. SEM image of LiFePO_4/C electrodes prepared using (a) aqueous binders of PTFE and (b) PVDF, as well as the electrodes combined with (c) aqueous binders of PTFE and (d) PVDF [58].

3.2. SF Binders of PTFE

Polymer fibrillation requires materials with unique characteristics. Currently, the most optimal selection for a binder is limited to PTFE due to its exceptional mechanical qualities, high crystallinity (achieving 97% or more post-sintering) [59][60][61], and its ability to produce fibers. PTFE exhibits flexibility and reduced resilience compared to the properties of other polymers, with moderate tensile strength and high elongation at the break [62][63]. The material undergoes deformation under specific pressure conditions, while retaining the correct dimensions. The above behavior perfectly matches the processing requirements for the SF method of electrode stretch molding.

3.2.1. Molecular Structure

PTFE possesses the highest chemical resistance, a high dielectric constant, and a wide range of operating temperatures [64]. The properties of PTFE result from its high crystallinity, high molecular weight, and unbranched structure. The radius of the F atom in PTFE is more significant than that of the H atom, and the C-F bonding energy is relatively vital (485 kJ mol^{-1}) [62][63][64][65]. Therefore, the adjacent $-\text{CF}_2-$ units in the molecular chain structure cannot present a transverse cross-orientation conformation, as does polyethylene, and instead appear to be helically arranged in the overall conformation [66]. This spiral arrangement of the F atoms surrounds the carbon main chain. It covers the entire surface of the molecular chain, forming a protective layer of low surface energy around the C-C main chain. This non-polar and inert dense layer produces high intermolecular van der Waals repulsion.

3.2.2. The Principle of Polymer Fibrillation

PTFE SF binder particles show an average particle size of $500 \mu\text{m}$, with many oblate spheroidal particles. These particles are comprised of several folded lamellar crystals ($0.54 \mu\text{m}$ long, $0.25 \mu\text{m}$ wide) [64][67]. When applying a shear load to PTFE, the oblate spheroidal particles exhibit flexibility, allowing them to elongate and form a fiber. This process is called “fibrillation” in **Figure 5a,b** [68].

Why can fibrillations occur using PTFE? There are two primary factors contributing to this phenomenon. One is the dislocation slip in the PTFE polymer crystals [69]. The polymer’s crystal structure determines the fibrillation behavior caused by dislocations. As shown in **Figure 5c**, the crystal structure of PTFE can be divided into four phases [70][71]: pseudo-hexagonal crystal (Phase I), trilobal crystal (Phase II), planar zig-zag crystal (Phase III), and hexagonal crystal (Phase IV). Taking the hexagonal crystals of Phase IV as an example, the pre-fibrillation operation in the range of $19\text{--}30^\circ\text{C}$ transforms the crystalline phase of PTFE from Phase II to Phase IV. The PTFE’s repeating distance along the molecular axis increases from 1.65 nm in the triple-diagonal crystals to 1.95 nm in the hexagonal crystals. Additionally, the repeating helical structure in the molecular chain expands $-\text{CF}_2-$ from 13 to 15, accompanied by a slight expansion in the structure of the helical repeating units [71]. The structure of the helical repeating unit is slightly expanded in **Figure 5d** [72]. In this phase of PTFE, the cohesion between the neighboring chains is weak and easily dislocated. In order to avoid polymer chain breakage, dislocations can generally only slide along planes parallel to the polymer chains, most commonly

observed as chain slip and lateral slip. The sliding deformation of PTFE along the chain (c-axis of the hexagonal system) has been reported to be easier to deform into nanofiber structures under a high aspect ratio, as shown in **Figure 5e** [72].

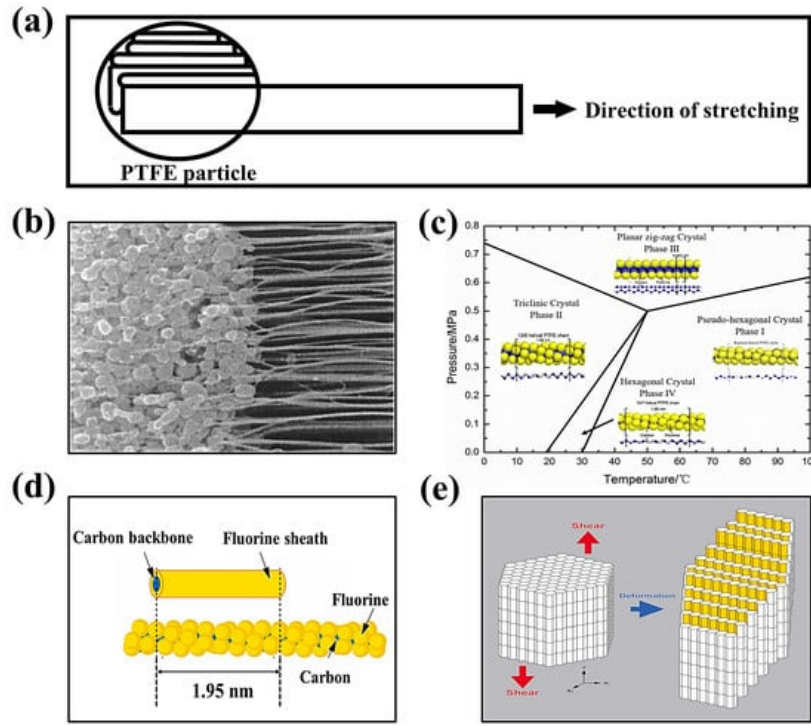


Figure 5. (a) PTFE spheres are stretched into banded fibers [68]. (b) SEM image (2 μm) of PTFE fibrillation [68]. (c) Phase diagram of PTFE [74]. (d) The individual PTFE polymer chain with helical structure and its simplified cylinder model [72]. (e) The PTFE crystals with slip dislocations occurring under shear [72].

3.2.3. Factors Affecting PTFE Fibrillation

Currently, there are fewer studies dedicated to discussing the influence of fibrillation properties. In the field of SF batteries research, Maxwell's experimental data show that the impedance of the original fibrillated electrode film is related to the feed rate and the shear force [73]. Related reports in other fields also assist in investigating the mechanical behavior of PTFE. Aimin Zhang et al. [74] explored the fibrillation mechanism, crystallization behavior, and mechanical properties of in situ fiber PTFE-reinforced PP composites. The experimental results showed that the shear rate is the key parameter affecting the morphological evolution of PTFE, and the processing time also affects the morphology of PTFE, to a certain extent.

The influencing factor of PTFE deformation may consist of a single variable or a synergistic effect of multiple variables. As a binder in polymer fibrillation, PTFE should possess a smaller particle size and a higher molecular weight.

4. SF Process with PTFE Binder

4.1. Positive Characteristics

Figure 6a shows a comparison of the wet and dry processes, and **Figure 6b** shows the SEM images of the electrodes for the wet and dry processes (polymer fibrillation). Polymer fibrillation stands out in the SF approach to batteries because of the following five advantages.

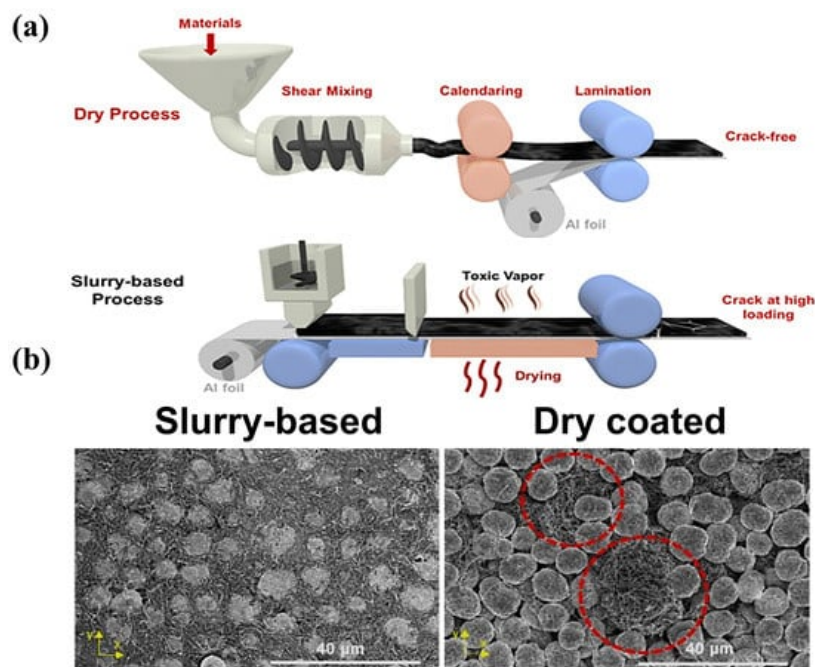


Figure 6. (a) Scheme of the PTFE-based SF and SC processes [75]; (b) the top surface of slurry-based LNMO electrodes and SF coated electrodes [75].

I. It is environmentally friendly and suitable for large-scale production.

NMP solvent is toxic, unfriendly to the environment, and needs to be recycled using the traditional wet process. The SF process does not require solvent in the electrode coating process to reduce baking and solvent recovery, the process is simpler, the equipment covers a smaller area, and the method is more suitable for the large-scale production of electrodes.

II. It exhibits a flatter electrode shape than that from the wet process.

Because the wet method requires solvent, after the solvent evaporation, the active substance and conductive agent will leave more spaces between the gaps, leading to the low compaction density of the material. The SF method does not exist in the drying process, so there is no solvent evaporation left after the gap, and the contact between the particles is closer.

III. It offers greater compaction density.

After compaction under dry conditions, there are fewer cracks, micropores, and other problems. The compacted density of lithium iron phosphate and SF battery energy density may be improved. According to Maxwell's experimental data [73], the energy density of the SF electrode can be more than 300 Wh/kg, and has the possibility to realize 500 Wh/kg.

IV. It improves the performance of the battery

In the wet process, after the battery has gone through many cycles, the stresses within the active particles continue to accumulate, leading to cracks in the profile, which ultimately reduces the performance of the battery. In the SF process, the fiber network is wrapped around the surface of the active material, and the mesh structure remains intact after many cycles of charging and discharging.

V. It allows for the possibility of prepare solid-state batteries.

Empowered by SF technology, the manufacturing process for creating solid-state battery electrodes can be completely dried, eliminating the problem of solvent molecules remaining after drying in the wet process. In addition, the use of the original fibrillation manufacturing solid electrolyte film can reduce manufacturing costs so that solid-state batteries can also be more productive.

4.2. Development Status of SF Process with PTFE Binder

4.2.1. Effect of PTFE on SF Batteries

The properties of PTFE determine the performance of the solvent-free batteries and influence the SF process at the fundamental level. Relevant studies have been devoted to exploring whether changing the PTFE has an impact on the battery system, and the standard variables include the side reactions of positive and negative electrodes, ultra-low content (0.1–0.5 wt%), crystallinity, modified molecules of PTFE, substitutes for PTFE, and synergistic polymer binder.

I. Side reactions of PTFE binders

The reaction between PTFE and Li^+ on the surface of the negative electrode will preferentially react to generate lithium fluoride, weakening the bonding effect and even destroying the PTFE electrode fiber network, leading to a rapid decline in electrode performance. This phenomenon was reported by Wu et al. in 2019 [76]. The chemical reaction between PTFE and Li^+ can cause a low initial reversible capacity (<70%) of the anode of the $\text{LiNi}_{0.6}\text{Mn}_{0.2}\text{Co}_{0.2}\text{O}_2$ (NMC622)/graphite full battery. Chen's group raised This problem as early as 1996 [77].

Does PTFE reveal a similar problem in the cathode? In 2023, Tao et al. [78] compared the changes in the batteries' cathode electrolyte interface layer (CEI) using electrolytes containing LiPF_6 or LiClO_4 . Using LiClO_4 can eliminate other possible F sources, thereby probing the decomposition of PTFE.

II. Crystallinity

In addition to the PTFE content, the crystallinity also affects the SF procedure. To investigate the effect of PTFE crystallinity on all-solid-state batteries (ASSBs), a class of sulfide-based $\text{Li}_6\text{PS}_5\text{Cl}$ -ASSBs was constructed by Dongsoo Lee [67] in 2023. The PTFE formulations used in this experiment were non-crystalline (18.8%), semi-crystalline (41.3%), and highly crystalline (88.1%), respectively. The high crystallinity PTFE exhibited more substantial mechanical properties and closer contact with the active substance particles. Because it promotes uniform charge transfer in the battery, this PTFE can significantly improve the performance of ASSBs.

III. Modified materials

Battery-grade PTFE exhibits the limitation of being difficult to store. Previous studies have attempted to modify or replace PTFE. In 2022, Hong et al. [79] developed a modified PTFE material: poly (tetrafluoroethylene-co-perfluoro (3-oxo-4-pentanesulfonic acid)) lithium. The cross-sectional SEM images of the cathode without adhesive, containing PTFE and the ionic polymer, are shown in **Figure 7**.

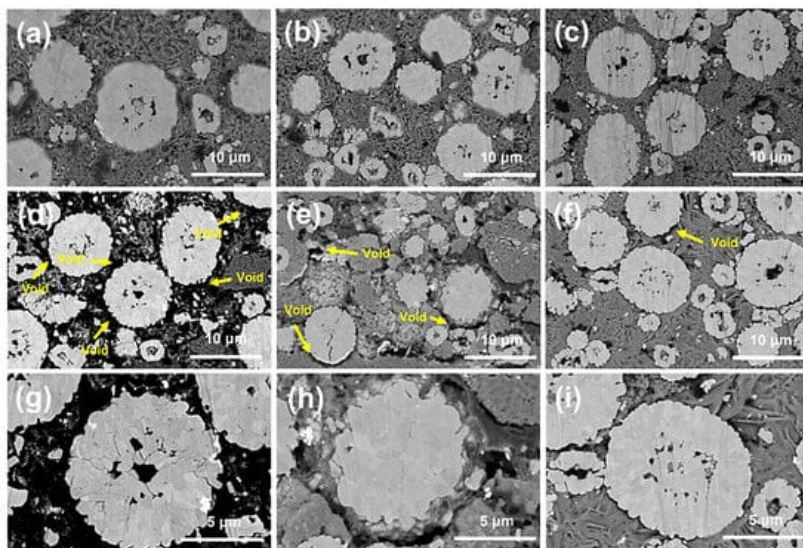


Figure 7. Cross-sectional SEM images of cathodes prepared (a) without binder, (b) with PTFE, and (c) with the ionic polymer. Cross-sectional SEM images of cycled (300 cycles) cathodes prepared (d,g) without binder, (e,h) with PTFE, and (f,i) with the ionic polymer [79].

4.2.2. Influence of Components Other Than Binders

I. Conductive additives

For the variable of conductive additives, in 2023, Yang et al. [80] prepared a full battery, with different carbon active materials (graphite, stiff carbon, and soft carbon) as the negative electrode, and $\text{LiNi}_{0.5}\text{Co}_{0.2}\text{Mn}_{0.3}\text{O}_2$ as the positive electrode. As shown in **Figure 8a**, the hard and soft carbon negative electrodes exhibited better cycling stability than that

of graphite due to their small volume expansion during charge storage, and this work successfully expanded the application scope of the PTFE-based SF process. Their group also investigated similar work, as shown in **Figure 8b** [81].

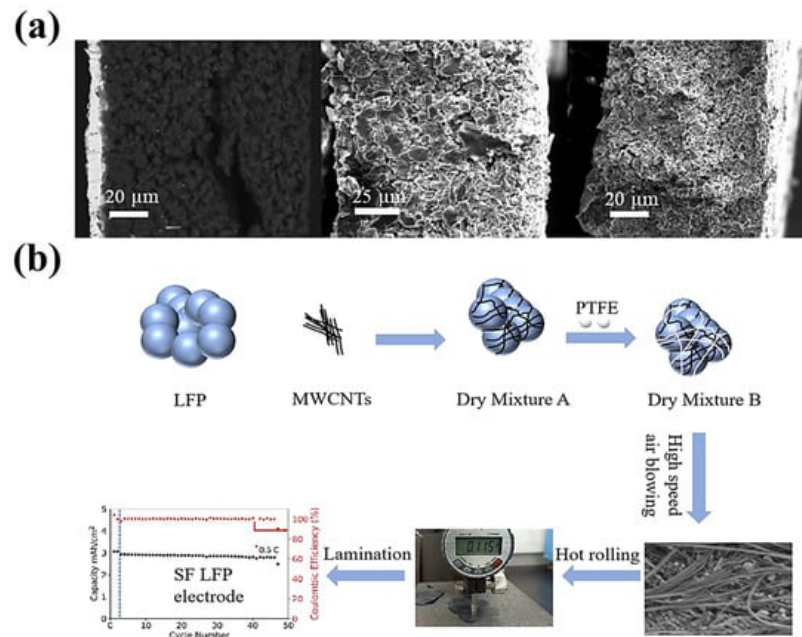


Figure 8. (a) Cross-sectional SEM images of a graphite, hard carbon, and soft carbon SF anode [79]. (b) SF-LFP electrode procedure [81].

II. Electrode materials

The electrode material will not only have an effect on the SF electrode method alone, but it will also affect the overall capacity of the SF batteries. For SF electrode technology, measures such as developing electrode materials with higher specific capacity, increasing the proportion of active substances, and selecting active substances in the appropriate voltage range could enhance the overall performance of the SF batteries. Based on the method using the PTFE solvent-free electrode to adjust for the variation of other components, it will be expected to obtain higher performance batteries. This means that there is an excellent opportunity to prepare high-capacity batteries from the perspective of the PTFE solvent-free process.

III. Collectors

Although there are previous works reporting on collector-free LIBs, most of them focus on the design of an integrated battery structure concept. Currently, the SF batteries usually obtained using the polymer fibrillation method use temperatures of 180 °C and above [] to hot press and hold electrode self-supporting film for a period of time, while employing collectors such as aluminum foil, copper foil, carbon coated aluminum foil, etc.

4.2.3. Innovative Technology and System

The exploration of battery processes and systems is also essential. Nevertheless, several efforts have also focused on novel SF battery systems, such as those involving high-voltage, solid-state, and high-load battery systems.

I. High-speed airflow technology

In 2020, Zhou et al. [82] used a high-speed airflow impact to defibrillate PTFE, along with the use of conductive additives and the inclusion of active materials. Subsequently, they successfully prepared SF-LFP electrodes by combining hot rolling and hot covering processes.

II. Lithium-sulfur (Li-S) batteries

In 2023, Magdalena et al. [83] achieved the preparation of SF all-solid-state lithium-sulfur batteries with high sulfur utilization (ASSB-LiS) by using a high-energy ball milling method. The group pioneered the monitoring of the thickness of ASSB-LiS electrode sheets prepared using the SF process. This approach enabled a deeper understanding of the charging and discharging behavior of ASSB-LiS.

III. High-voltage batteries

High-voltage batteries are crucial for the development of the sustainable LIBs market. Moreover, high-voltage cobalt-free batteries with high energy density and low cost-effectiveness offer new possibilities for the battery industry. In 2023, Yao et al. [75] developed a 5V-grade cobalt-free battery based on a PTFE-based SF process, which enabled the successful preparation of a highly loaded spinel-type oxide $\text{LiNi}_{0.5}\text{Mn}_{1.5}\text{O}_4$ (LNMO) electrode. The wet electrode surface loading performance starts to decrease at 4.0 mAh cm^{-2} . However, the battery electrochemical performance continues to remain stable up to 9.5 mAh cm^{-2} ($240 \text{ }\mu\text{m}$ thick) of the SF electrode.

IV. High-load batteries

In 2023, Tao et al. [84] constructed a whole battery consisting of a highly loaded graphite (6.6 mAh cm^{-2}) as the negative electrode and $\text{LiNi}_{0.6}\text{Mn}_{0.2}\text{Co}_{0.2}\text{O}_2$ (6.0 mAh cm^{-2}) as the positive electrode by using PTFE as the binder using the SF process in order to compare it with the wet approach. The SF procedure exhibits significant advantages over the SC process in regards to multiplication performance and capacity retention for the entire battery.

V. Solid-state batteries

The development of the SF-solid-state battery system should not be underestimated. Dong et al. [85] investigated the factors affecting the performance of SF solid-state batteries by exploring the content of the cathode active material and the solid electrolytes. The data from the batteries show that the most critical design criterion for SF solid-state batteries is the need for a reasonable and balanced conduction path in the SF composite electrode.

References

1. Dang, C.C.; Mu, Q.; Xie, X.B.; Sun, X.Q.; Yang, X.Y.; Zhang, Y.P.; Maganti, S.; Huang, M.N.; Jiang, Q.L.; Seok, I.; et al. Recent Progress in Cathode Catalyst for Nonaqueous Lithium Oxygen Batteries: A review. *Adv. Compos. Hybrid Mater.* 2022, 5, 606–626.
2. Eng, A.Y.S.; Soni, C.B.; Lum, Y.; Khoo, E.; Yao, Z.; Vineeth, S.K.; Kumar, V.; Lu, J.; Johnson, C.S.; Wolverton, C.; et al. Theory-Guided Experimental Design in Battery Materials Research. *Sci. Adv.* 2022, 8, eabm2422.
3. Jiang, M.; Danilov, D.L.; Eichel, R.A.; Notten, P.H.L. A Review of Degradation Mechanisms and Recent Achievements for Ni-Rich Cathode-Based Li-Ion Batteries. *Adv. Energy Mater.* 2021, 11, 2103005.
4. Kalnaus, S.; Dudney, N.J.; Westover, A.S.; Herbert, E.; Hackney, S. Solid-State Batteries: The Critical Role of Mechanics. *Science* 2023, 381, eabg5998.
5. Li, J.L.; Fleetwood, J.; Hawley, W.B.; Kays, W. From Materials to Cell: State-of-the-Art and Prospective Technologies for Lithium-Ion Battery Electrode Processing. *Chem. Rev.* 2022, 122, 903–956.
6. Liu, W.; Placke, T.; Chau, K.T. Overview of Batteries and Battery Management for Electric Vehicles. *Energy Rep.* 2022, 8, 4058–4084.
7. Wang, W.; Yuan, B.Q.; Sun, Q.; Wennersten, R. Application of Energy Storage in Integrated Energy Systems-A Solution to Fluctuation and Uncertainty of Renewable Energy. *J. Energy Storage* 2022, 52, 104812.
8. Viswanathan, V.; Epstein, A.H.; Chiang, Y.M.; Takeuchi, E.; Bradley, M.; Langford, J.; Winter, M. The Challenges and Opportunities of Battery-Powered Flight. *Nature* 2022, 601, 519–525.
9. Xing, C.W.; Li, M.C.; Liu, L.Y.; Lu, R.; Liu, N.; Wu, W.J.; Yuan, D.D. A Comprehensive Review on the Blending Condition Between Virgin and RAP Asphalt Binders in Hot Recycled Asphalt Mixtures: Mechanisms, Evaluation Methods, and Influencing Factors. *J. Clean. Prod.* 2023, 398, 136515.
10. Zhu, C.; Usiskin, R.E.; Yu, Y.; Maier, J. The Nanoscale Circuitry of Battery Electrodes. *Science* 2017, 358, eaao2808.
11. Ludwig, A.; Wu, M.; Kharicha, A. On The Importance of Modeling 3D Shrinkage Cavities for the Prediction of Macrosegregation in Steel Ingots. *CFD Model. Simu. Mat. Pro.* 2016, 2016, 1–10.
12. Pillai, A.M.; Salini, P.S.; John, B.; Devassy, M.T. Aqueous Binders for Cathodes: A Lodestar for Greener Lithium Ion Cells. *Energy Fuels* 2022, 36, 5063–5087.
13. Guo, R.N.; Han, W.Q. Effects of Structure and Properties of Polar Polymeric Binders on Lithium-ion Batteries. *Inorg. Mater.* 2019, 34, 1021–1029.
14. Wang, Y.B.; Yang, Q.; Guo, X.; Yang, S.; Chen, A.; Liang, G.J.; Zhi, C.Y. Strategies of Binder Design for High-Performance Lithium-Ion Batteries: A Mini Review. *Rare Metals* 2022, 41, 745–761.

15. Pettinger, K.-H.; Dong, W. When Does the Operation of a Battery Become Environmentally Positive? *J. Electrochem. Soc.* 2017, 164, A6274.
16. Al-Shroofy, M.; Zhang, Q.; Xu, J.; Chen, T.; Kaur, A.P.; Cheng, Y.-T. Solvent-Free Dry Powder Coating Process for Low-Cost Manufacturing of $\text{LiNi}_{1/3}\text{Mn}_{1/3}\text{Co}_{1/3}\text{O}_2$ Cathodes in Lithium-Ion Batteries. *J. Power Sources* 2017, 352, 187–193.
17. Ludwig, B.; Liu, J.; Chen, I.M.; Liu, Y.; Shou, W.; Wang, Y.; Pan, H. Understanding Interfacial-Energy-Driven Dry Powder Mixing for Solvent-Free Additive Manufacturing of Li-Ion Battery Electrodes. *Ad. Mater. Interfaces* 2017, 4, 1700570.
18. Shiraki, S.; Oki, H.; Takagi, Y.; Suzuki, T.; Kumatani, A.; Shimizu, R.; Haruta, M.; Ohsawa, T.; Sato, Y.; Ikuhara, Y.; et al. Fabrication of All-Solid-State Battery Using Epitaxial LiCoO_2 Thin Films. *J. Power Sources* 2014, 267, 881–887.
19. Subramanyam, G.; Cole, M.W.; Sun, N.X.; Kalkur, T.S.; Sbrokeky, N.M.; Tompa, G.S.; Guo, X.; Chen, C.; Alpay, S.P.; Rossetti, G.A.; et al. Challenges and Opportunities for Multi-Functional Oxide Thin Films for Voltage Tunable Radio Frequency/Microwave Components. *J. Appl. Phys.* 2013, 114, 191301.
20. Sotomayor, M.E.; Torre-Gamarra, C.d.I.; Levenfeld, B.; Sanchez, J.-Y.; Varez, A.; Kim, G.-T.; Varzi, A.; Passerini, S. Ultra-Thick Battery Electrodes for High Gravimetric and Volumetric Energy Density Li-Ion Batteries. *J. Power Sources* 2019, 437, 226923.
21. Trembacki, B.; Duoss, E.; Oxberry, G.; Stadermann, M.; Murthy, J. Mesoscale Electrochemical Performance Simulation of 3D Interpenetrating Lithium-Ion Battery Electrodes. *J. Electrochem. Soc.* 2019, 166, A923.
22. Carneiro, O.S.; Silva, A.F.; Gomes, R. Fused Deposition Modeling with Polypropylene. *Mater. Des.* 2015, 83, 768–776.
23. Kirsch, D.J.; Lacey, S.D.; Kuang, Y.; Pastel, G.; Xie, H.; Connell, J.W.; Lin, Y.; Hu, L. Scalable Dry Processing of Binder-Free Lithium-Ion Battery Electrodes Enabled by Holey Graphene. *ACS Appl. Energy Mater.* 2019, 2, 2990–2997.
24. Han, X.; Funk, M.R.; Shen, F.; Chen, Y.-C.; Li, Y.; Campbell, C.J.; Dai, J.; Yang, X.; Kim, J.W.; Liao, Y.; et al. Scalable Holey Graphene Synthesis and Dense Electrode Fabrication toward High-Performance Ultracapacitors. *ACS Nano* 2014, 8, 8255–8265.
25. Lee, D.J.; Jang, J.; Lee, J.-P.; Wu, J.; Chen, Y.-T.; Holoubek, J.; Yu, K.; Ham, S.-Y.; Jeon, Y.; Kim, T.-H.; et al. Physio-Electrochemically Durable Dry-Processed Solid-State Electrolyte Films for All-Solid-State Batteries. *Adv. Funct. Mater.* 2023, 33, 2301341.
26. Wood, D.L.; Wood, M.; Li, J.; Du, Z.; Ruther, R.E.; Hays, K.A.; Muralidharan, N.; Geng, L.; Mao, C.; Belharouak, I. Perspectives on The Relationship Between Materials Chemistry and Roll-to-Roll Electrode Manufacturing for High-Energy Lithium-Ion Batteries. *Energy Stor. Mater.* 2020, 29, 254–265.
27. Ludwig, B.; Zheng, Z.; Shou, W.; Wang, Y.; Pan, H. Solvent-Free Manufacturing of Electrodes for Lithium-ion Batteries. *Sci. Rep.* 2016, 6, 23150.
28. Li, Y.; Wu, Y.; Wang, Z.; Xu, J.; Ma, T.; Chen, L.; Li, H.; Wu, F. Progress in Solvent-Free Dry-Film Technology for Batteries and Supercapacitors. *Mater. Today* 2022, 55, 92–109.
29. Lu, Y.; Zhao, C.-Z.; Yuan, H.; Hu, J.-K.; Huang, J.-Q.; Zhang, Q. Dry Electrode Technology, The Rising Star in Solid-state Battery Industrialization. *Matter* 2022, 5, 876–898.
30. Zou, F.; Manthiram, A. A Review of the Design of Advanced Binders for High-Performance Batteries. *Adv. Energy Mater.* 2020, 10, 2002508.
31. Wu, Y.; Li, Y.; Wang, Y.; Liu, Q.; Chen, Q.; Chen, M. Advances and Prospects of PVDF Based Polymer Electrolytes. *J. Energy Chem.* 2022, 64, 62–84.
32. Zhu, T.; Sternlicht, H.; Ha, Y.; Fang, C.; Liu, D.; Savitzky, B.H.; Zhao, X.; Lu, Y.; Fu, Y.; Ophus, C.; et al. Formation of Hierarchically Ordered Structures in Conductive Polymers to Enhance the Performances of Lithium-Ion Batteries. *Nat. Energy* 2023, 8, 129–137.
33. Oh, J.; Choi, S.H.; Chang, B.; Lee, J.; Lee, T.; Lee, N.; Kim, H.; Kim, Y.; Im, G.; Lee, S.; et al. Elastic Binder for High-Performance Sulfide-Based All-Solid-State Batteries. *ACS Energy Lett.* 2022, 7, 1374–1382.
34. Mu, P.; Zhang, H.; Jiang, H.; Dong, T.; Zhang, S.; Wang, C.; Li, J.; Ma, Y.; Dong, S.; Cui, G. Bioinspired Antiaging Binder Additive Addressing the Challenge of Chemical Degradation of Electrolyte at Cathode/Electrolyte Interphase. *J. Am. Chem. Soc.* 2021, 143, 18041–18051.
35. Maleki, H.; Deng, G.; Kerzhner-Haller, I.; Anani, A.; Howard, J.N. Thermal Stability Studies of Binder Materials in Anodes for Lithium-Ion Batteries. *J. Electrochem. Soc.* 2000, 147, 4470.

36. Yonaga, A.; Kawauchi, S.; Mori, Y.; Xuanchen, L.; Ishikawa, S.; Nunoshita, K.; Inoue, G.; Matsunaga, T. Effects of Dry Powder Mixing on Electrochemical Performance of Lithium-ion Battery Electrode Using Solvent-Free Dry Forming Process. *J. Power Sources* 2023, 581, 233466.
37. Zhang, Z.; Han, D.; Xiao, M.; Wang, S.; Feng, Y.; Huang, S.; Meng, Y. New Potential Substitute of PVDF Binder: Poly(propylene carbonate) for Solvent-Free Manufacturing High-Loading Cathodes of LiFePO₄|Li Batteries. *Ionics* 2023, 29, 3895–3906.
38. Abdel-Hakim, A.; El-Basheer, T.M.; Abdelkhalik, A. Mechanical, Acoustical and Flammability Properties of SBR and SBR-PU Foam Layered Structure. *Poly. Test.* 2020, 88, 106536.
39. Li, Y.; Wu, Y.; Ma, T.; Wang, Z.; Gao, Q.; Xu, J.; Chen, L.; Li, H.; Wu, F. Long-Life Sulfide All-Solid-State Battery Enabled by Substrate-Modulated Dry-Process Binder. *Adv. Energy Mater.* 2022, 12, 2201732.
40. Park, J.; Willenbacher, N.; Ahn, K.H. How the Interaction Between Styrene-Butadiene-Rubber (SBR) Binder and a Secondary Fluid Affects the Rheology, Microstructure and Adhesive Properties of Capillary-Suspension-Type Graphite Slurries Used for Li-ion Battery Anodes. *Colloids Surf. A Physicochem. Eng. Asp.* 2019, 579, 123692.
41. Dueramae, I.; Okhawilai, M.; Kasemsiri, P.; Uyama, H.; Kita, R. Properties Enhancement of Carboxymethyl Cellulose with Thermo-Responsive Polymer as Solid Polymer Electrolyte for Zinc Ion Battery. *Sci. Rep.* 2020, 10, 12587.
42. Kim, J.; Choi, J.; Park, K.; Kim, S.; Nam, K.W.; Char, K.; Choi, J.W. Host–Guest Interlocked Complex Binder for Silicon–Graphite Composite Electrodes in Lithium Ion Batteries. *Adv. Energy Mater.* 2022, 12, 2103718.
43. Ibrahim, S.M.; El Salmawi, K.M. Preparation and Properties of Carboxymethyl Cellulose (CMC)/Sodium alginate (SA) Blends Induced by Gamma Irradiation. *J. Polym. Environ.* 2013, 21, 520–527.
44. Xu, Z.; Yang, J.; Zhang, T.; Nuli, Y.; Wang, J.; Hirano, S.-i. Silicon Microparticle Anodes with Self-Healing Multiple Network Binder. *Joule* 2018, 2, 950–961.
45. Hu, Y.; Shao, D.; Chen, Y.; Peng, J.; Dai, S.; Huang, M.; Guo, Z.-H.; Luo, X.; Yue, K. A Physically Cross-Linked Hydrogen-Bonded Polymeric Composite Binder for High-Performance Silicon Anodes. *ACS Appl. Energy Mater.* 2021, 4, 10886–10895.
46. Senthil, C.; Kim, S.-S.; Jung, H.Y. Flame Retardant High-Power Li-S Flexible Batteries Enabled by Bio-macromolecular Binder Integrating Conformal Fractions. *Nat. Commun.* 2022, 13, 145.
47. Mackanic, D.G.; Yan, X.; Zhang, Q.; Matsuhisa, N.; Yu, Z.; Jiang, Y.; Manika, T.; Lopez, J.; Yan, H.; Liu, K.; et al. Decoupling of Mechanical Properties and Ionic Conductivity in Supramolecular Lithium Ion Conductors. *Nat. Commun.* 2019, 10, 5384.
48. Dong, T.; Zhang, H.; Hu, R.; Mu, P.; Liu, Z.; Du, X.; Lu, C.; Lu, G.; Liu, W.; Cui, G. A Rigid-Flexible Coupling Poly (vinylene carbonate) Based Cross-Linked Network: A versatile Polymer Platform for Solid-state Polymer Lithium Batteries. *Energy Stor. Mater.* 2022, 50, 525–532.
49. Xia, J.; Wang, Z.; Rodrig, N.D.; Nan, B.; Zhang, J.; Zhang, W.; Lucht, B.L.; Yang, C.; Wang, C. Super-Reversible CuF₂ Cathodes Enabled by Cu²⁺-Coordinated Alginate. *Adv. Mater.* 2022, 34, 2205229.
50. Jeong, Y.K.; Kwon, T.-w.; Lee, I.; Kim, T.-S.; Coskun, A.; Choi, J.W. Millipede-inspired structural design principle for high performance polysaccharide binders in silicon anodes. *Energy Environ. Sci.* 2015, 8, 1224–1230.
51. Strand, A.; Kouko, J.; Oksanen, A.; Salminen, K.; Ketola, A.; Retulainen, E.; Sundberg, A. Enhanced Strength, Stiffness and Elongation Potential of Paper by Spray Addition of Polysaccharides. *Cellulose* 2019, 26, 3473–3487.
52. Qin, T.; Yang, H.; Li, Q.; Yu, X.; Li, H. Design of Functional Binders for High-Specific-Energy Lithium-Ion Batteries: From Molecular Structure to Electrode Properties. *Ind. Eng. Chem. Res.* 2023.
53. Wang, X.; Liu, S.; Zhang, Y.; Wang, H.; Aboalhassan, A.A.; Li, G.; Xu, G.; Xue, C.; Yu, J.; Yan, J.; et al. Highly Elastic Block Copolymer Binders for Silicon Anodes in Lithium-Ion Batteries. *ACS Appl. Mater. Interfaces* 2020, 12, 38132–38139.
54. Ignatieva, L.N.; Mashchenko, V.A.; Zverev, G.A.; Ustinov, A.Y.; Slobodyuk, A.B.; Bouznik, V.M. Study of The Manufactured Copolymers of Ethylene with Tetrafluoroethylene. *J. Fluor. Chem.* 2020, 231, 109460.
55. Zhang, Y.; Lu, S.; Wang, Z.; Volkov, V.; Lou, F.; Yu, Z. Recent Technology Development in Solvent-Free Electrode Fabrication for Lithium-Ion Batteries. *Renew. Sust. Energ. Rev.* 2023, 183, 113515.
56. Huang, S.; Huang, X.T.; Huang, Y.Y.; He, X.Q.; Zhuo, H.T.; Chen, S.J. Rational Design of Effective Binders for LiFePO₄ Cathodes. *Polymers* 2021, 13, 3146.
57. Liu, Y.; Zhang, R.; Wang, J.; Wang, Y. Current and Future Lithium-Ion Battery Manufacturing. *iScience* 2021, 24, 102332.

58. Gao, S.; Su, Y.; Bao, L.; Li, N.; Chen, L.; Zheng, Y.; Tian, J.; Li, J.; Chen, S.; Wu, F. High-Performance LiFePO₄/C Electrode with Polytetrafluoroethylene as An Aqueous-Based Binder. *J. Power Sources* 2015, 298, 292–298.
59. Li, W.; Mays, S.; Lam, D. Material and Finite Element Analysis of Poly(tetrafluoroethylene) O-ring Seals. *Plast. Rubber Compos.* 2002, 31, 359–363.
60. Brown, E.N.; Rae, P.J.; Bruce Orler, E.; Gray, G.T.; Dattelbaum, D.M. The Effect of Crystallinity on the Fracture of Polytetrafluoroethylene (PTFE). *Mater. Sci. Eng. C* 2006, 26, 1338–1343.
61. Brown, E.N.; Dattelbaum, D.M. The Role of Crystalline Phase on Fracture and Microstructure Evolution of Polytetrafluoroethylene (PTFE). *Polymer* 2005, 46, 3056–3068.
62. Joyce, J.A. Fracture Toughness Evaluation of Polytetrafluoroethylene. *Polym. Eng. Sci.* 2003, 43, 1702–1714.
63. Rae, P.J.; Brown, E.N. The Properties of Poly(tetrafluoroethylene) (PTFE) in Tension. *Polymer* 2005, 46, 8128–8140.
64. Pruitt, L.A. Deformation, Yielding, Fracture and Fatigue Behavior of Conventional and Highly Cross-Linked Ultra High Molecular Weight Polyethylene. *Biomaterials* 2005, 26, 905–915.
65. Brown, E.N.; Trujillo, C.P.; Gray, G.T.; Rae, P.J.; Bourne, N.K. Soft Recovery of Polytetrafluoroethylene Shocked Through The Crystalline Phase II-III Transition. *J. Appl. Phys.* 2007, 101, 024916.
66. Millett, J.C.F.; Brown, E.N.; Gray, G.T.; Bourne, N.K.; Wood, D.C.; Appleby-Thomas, G. The Effects of Changing Chemistry on the Shock Response of Basic Polymers. *J. Dyn. Behav. Mater.* 2016, 2, 326–336.
67. Lee, D.; Manthiram, A. Stable Cycling with Intimate Contacts Enabled by Crystallinity-Controlled PTFE-Based Solvent-Free Cathodes in All-Solid-State Batteries. *Small Methods* 2023, 7, 2201680.
68. Kitamura, T.; Okabe, S.; Tanigaki, M.; Kurumada, K.; Ohshima, M.; Kanazawa, S. Morphology Change in Polytetrafluoroethylene (PTFE) Porous Membrane Caused by Heat Treatment. *Polym. Eng. Sci.* 2000, 40, 809–817.
69. Wecker, S.M.; Davidson, T.; Baker, D.W. Preferred Orientation of Crystallites in Uniaxially Deformed Polytetrafluoroethylene. *J. Appl. Phys.* 1972, 43, 4344–4348.
70. Puts, G.J.; Crouse, P.; Ameduri, B.M. Polytetrafluoroethylene: Synthesis and Characterization of the Original Extreme Polymer. *Chem. Rev.* 2019, 119, 1763–1805.
71. Wu, J.; Wang, H.; Feng, B.; Li, Y.; Wu, S.; Yin, Q.; Yu, Z.; Huang, J. The Effect of Temperature-Induced Phase Transition of PTFE on The Dynamic Mechanical Behavior and Impact-Induced Initiation Characteristics of Al/PTFE. *Polym. Test.* 2020, 91, 106835.
72. Sato, K.; Tominaga, Y.; Imai, Y.; Yoshiyama, T.; Aburatani, Y. Deformation Capability of Poly(tetrafluoroethylene) Materials: Estimation with X-ray Diffraction Measurements. *Polym. Test* 2022, 113, 107690.
73. Hieu, D.; Joon, S.; Yudi, Y. Dry Electrode Coating Technology; Maxwell Technologies: San Diego, CA, USA, 2018; Available online: <https://api.semanticscholar.org/CorpusID:201928996> (accessed on 19 October 2023).
74. Zhang, A.; Chai, J.; Yang, C.; Zhao, J.; Zhao, G.; Wang, G. Fibrosis Mechanism, Crystallization Behavior and Mechanical Properties of In-Situ Fibrillary PTFE Reinforced PP Composites. *Mater. Des.* 2021, 211, 110157.
75. Yao, W.; Chouchane, M.; Li, W.; Bai, S.; Liu, Z.; Li, L.; Chen, A.X.; Sayahpour, B.; Shimizu, R.; Raghavendran, G.; et al. A 5 V-Class Cobalt-Free Battery Cathode with High Loading Enabled by Dry Coating. *Energy Environ. Sci.* 2023, 16, 1620–1630.
76. Wu, Q.; Zheng, J.P.; Hendrickson, M.; Plichta, E.J. Dry Process for Fabricating Low Cost and High Performance Electrode for Energy Storage Devices. *MRS Adv.* 2019, 4, 857–863.
77. Li, G. The Influence of Polytetrafluoroethylene Reduction on the Capacity Loss of the Carbon Anode for Lithium Ion Batteries. *Solid State Ion.* 1996, 90, 221–225.
78. Tao, R.; Tan, S.; Meyer Iii, H.M.; Sun, X.-G.; Steinhoff, B.; Sardo, K.; Bishtawi, A.; Gibbs, T.; Li, J. Insights into the Chemistry of the Cathodic Electrolyte Interphase for PTFE-Based Dry-Processed Cathodes. *ACS Appl. Mater. Interfaces* 2023, 15, 40488–40495.
79. Hong, S.B.; Lee, Y.J.; Kim, U.H.; Bak, C.; Lee, Y.M.; Cho, W.; Hah, H.J.; Sun, Y.K.; Kim, D.W. All-Solid-State Lithium Batteries: Li⁺-Conducting Ionomer Binder for Dry-Processed Composite Cathodes. *ACS Energy Letter* 2022, 7, 1092–1100.
80. Zhang, Y.; Huld, F.; Lu, S.; Jektvik, C.; Lou, F.; Yu, Z. Revisiting Polytetrafluoroethylene Binder for Solvent-Free Lithium-Ion Battery Anode Fabrication. *Batteries* 2022, 8, 57.
81. Zhang, Y.; Lu, S.; Lou, F.; Yu, Z. Solvent-free Lithium Iron Phosphate Cathode Fabrication with Fibrillation of Polytetrafluoroethylene. *Electrochim. Acta* 2023, 456, 142469.

82. Zhou, H.; Liu, M.; Gao, H.; Hou, D.; Yu, C.; Liu, C.; Zhang, D.; Wu, J.-C.; Yang, J.; Chen, D. Dense Integration of Solvent-Free Electrodes for Li-Ion Supercapattery with Boosted Low Temperature Performance. *J. Power Sources* 2020, 473, 228553.
83. Fiedler, M.; Cangaz, S.; Hippauf, F.; Dörfler, S.; Abendroth, T.; Althues, H.; Kaskel, S. Mechanistic Insights into the Cycling Behavior of Sulfur Dry-Film Cathodes. *Adv. Sustain. Syst.* 2023, 7, 2200439.
84. Tao, R.; Steinhoff, B.; Sun, X.-G.; Sardo, K.; Skelly, B.; Meyer, H.M.; Sawicki, C.; Polizos, G.; Lyu, X.; Du, Z.; et al. High-Throughput and High-performance Lithium-ion Batteries via Dry Processing. *Chem. Eng. J.* 2023, 471, 144300.
85. Shin, D.; Nam, J.S.; Linh Nguyen, C.T.; Jo, Y.; Lee, K.; Hwang, S.M.; Kim, Y.J. Design of Densified Nickel-Rich Layered Composite Cathode via The Dry-Film Process for Sulfide-Based Solid-State Batteries. *J. Mater. Chem. A* 2022, 10, 23222–23231.

Retrieved from <https://encyclopedia.pub/entry/history/show/119183>